Available online at www.sciencedirect.com
SCIENCE DIRECT®
Bioorganic & Medicinal Chemistry 14 (2006) 4089–4100
Bioorganic & Medicinal Chemistry

Binding of actinomycin C_1 (D) and actinomin to base-modified oligonucleotide duplexes with parallel chain orientation

Hong Li,[a] Xiaohua Peng,[a,b] Peter Leonard[b] and Frank Seela[a,b,*]

[a]*Laboratorium für Organische und Bioorganische Chemie, Institut für Chemie, Universität Osnabrück, Barbarastraße 7, 49069 Osnabrück, Germany*
[b]*Center for Nanotechnology, Gievenbecker Weg 11, 48149 Münster, Germany*

Received 4 November 2005; revised 1 February 2006; accepted 3 February 2006
Available online 24 February 2006

Abstract—The binding of actinomycin D (C_1, **1**) and its analog actinomin (**2**) was studied on base-modified oligonucleotide duplexes with parallel chain orientation (ps) and with anti-parallel chains (aps) for comparison. Actinomycin D binds not only to aps duplexes containing guanine–cytosine base pairs but also to those incorporating modified bases such as 7-deazaguanine or its 6-deoxo derivative. For this, novel phosphoramidites were prepared. The new building block of 7-deaza-2′-deoxyguanosine is significantly more stable than the one currently used and allows normal oxidation conditions during solid-phase oligonucleotide synthesis. Actinomycin binds weakly to ps duplexes containing guanine–isocytosine base pairs but not to ps-DNA incorporating pairs of isoguanine–cytosine residues. On the contrary, the actinomycin D analog actinomin, which contains positively charged side chains instead of the chiral peptide rings, is strongly bound to both ps- and aps-DNA. Guanines, isoguanine, as well as other 7-deaza derivatives are accepted as nucleobases. Apparently, the pentapeptide lacton rings of actinomycin do not fit nicely into the groove of ps-DNA thereby reducing the binding strength of the antibiotic while the groove size of ps-DNA does not affect actinomin binding notably.

1. Introduction

Parallel stranded (ps) DNA can be constructed from oligonucleotides incorporating isoguanine–cytosine or guanine–isocytosine base pairs instead of the canonical guanine–cytosine pair.[1–3] The dA–dT pair shows ambiguous base pairing and is accepted in anti-parallel stranded (aps) DNA as well as in ps-DNA.[4] In comparison, the ps-DNA contains grooves of about equal size.[4] Thus, the molecular recognition of ps-DNA by intercalating drugs or dyes might be different from DNA with anti-parallel chain orientation. As ps-DNA can offer new opportunities to design unique hybridization probes or antisense constructs,[5–8] the binding selectivity of ligands (dyes, antibiotics, etc.) is of interest.

The antibiotic actinomycin C_1 (D; **1**) is a widely studied ligand which binds to duplex DNA with anti-parallel chain orientation. It functions as an inhibitor of transcription both in vivo and in vitro, and results in anticancer activity, in particular against Hodgkin's disease.[9–11] The binding mode of actinomycin C_1 has been shown to be intercalative.[12] The chromophore inserts between the DNA base pairs, while the two pentapeptide lacton rings rest in the minor groove.[13–15] In general, the binding of **1** to DNA is sequence specific and requires dG–dC base pairs. Single crystal X-ray analysis of the DNA/drug complex shows that the structural basis for the dG–dC base pair selectivity is the formation of hydrogen bonds in the minor groove, between the 2-amino group or nitrogen-3 of two guanine residues, respectively, with the carbonyl oxygen atoms or amide groups of L-threonine residues of the pentapeptide lacton rings.[16–18] In this sense, the actinomycin–DNA complex can serve as a model for the highly specific conformational adaptation occurring between nucleic acids and peptides or proteins. As the resulting actinomycin–DNA complex occupies a four base pair duplex motif, the flanking residues to the binding site can modulate binding strength and the kinetics of binding.[19,20] Recently, the knowledge of actinomycin

Keywords: Actinomycin D; Actinomin; Base-modified nucleotides; Binding; Parallel DNA.
* Corresponding author. Tel.: +49 0 541 969 2791; fax: +49 0 541 969 2370; e-mail: Frank.Seela@uni-osnabrueck.de

0968-0896/$ - see front matter © 2006 Elsevier Ltd. All rights reserved.
doi:10.1016/j.bmc.2006.02.002

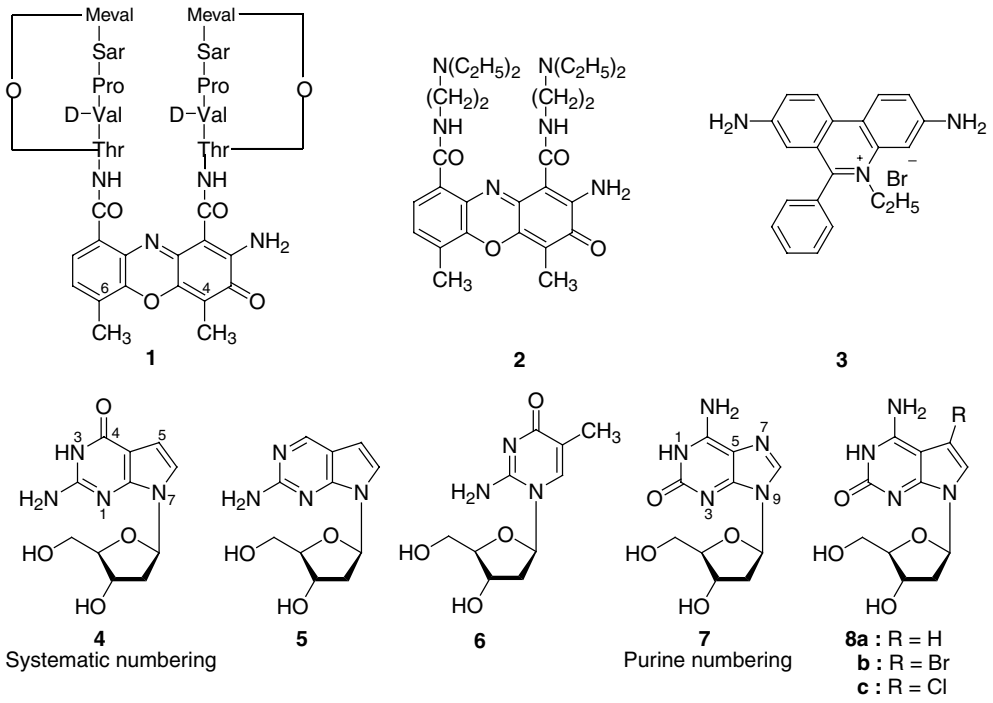

Scheme 1. Structures of compounds **1**–**8**.

binding to the observed dG–dC sequence preference of double-stranded DNA was extended to single-stranded DNAs.[21–24] Single-stranded DNA can form fold back structures resulting in hairpins, which bind actinomycin.[18,24] As the phenoxazone chromophore of actinomycin intercalates nicely between the tandem G · T mismatches, those hairpins containing G · T mismatches also bind actinomycin.[24]

This manuscript reports on the binding of actinomycin to parallel DNA. The parallel DNA contains $isoG_d$–dC or $isoC_d$–dG pairs along with reverse Watson Crick dA–dT pairs. Also the replacement of dG-residues by its 7-deazapurine derivative c^7G_d (**4**) or the 6-deoxo analog **5** and of $isoG_d$ (**7**) by the 7-deazapurine derivatives **8a**–**c** is investigated using the modified bases as chemical probes. The binding of actinomycin to ps duplexes is compared to those with anti-parallel chain orientation.

The studies were extended to the binding properties of the actinomycin D analog actinomin (**2**). This molecule represents a mimic of actinomycin in its ability to bind to DNA.[9,25,26] The pentapeptide lacton rings are replaced by aminotriethylamine residues which are positively charged under neutral conditions. Thus, the chiral recognition of the peptide moiety is mimicked by electrostatic forces formed with the negatively charged DNA phosphodiester backbone. Actinomin derivatives form dimers in aqueous solution[27] as it was observed for actinomycin D.[28,29] Within our studies visible and UV-spectroscopy, CD spectra, and fluorescent dye intercalator displacement (FID)[30] of ethidium bromide **3** as well as T_m-measurements are used to analyze the chiral and the non-chiral recognition of compounds **1** and **2** to ps- and aps-DNA.

2. Results and discussion

2.1. Synthesis of monomers

For the synthesis of phosphoramidites **11** and **14**, the corresponding nucleosides **5**[31] and **12**[32] were used as precursors. The amino group of compound **5** was protected with dimethylaminomethylidene group using dimethylformamide dimethylacetal in MeOH. Upon treatment with water the protecting group was degraded forming the 2-formyl derivative **9**. The latter was converted into

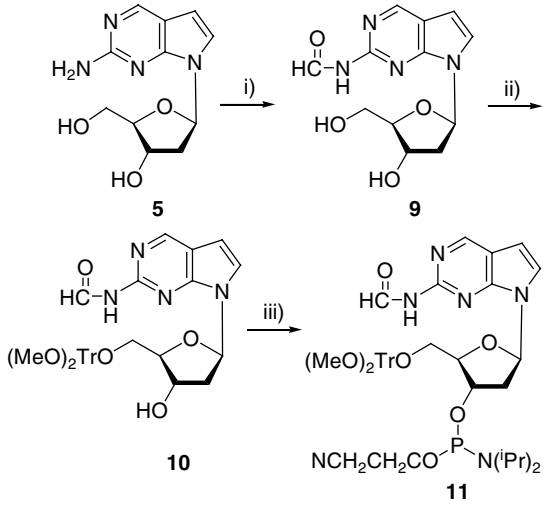

Scheme 2. Synthesis of compound **11**. Reagents and conditions: (i) a—*N*,*N*-dimethylformamide dimethylacetal, MeOH, 50 °C, 24 h; b—H_2O, 30–40 °C, 72 h; (ii) 4,4′-dimethoxytriphenylmethyl chloride, anhydrous pyridine, rt; (iii) 2-cyanoethyl-*N*,*N*-diisopropylchlorophosphoramidite, *N*,*N*-diisopropylethylamine, CH_2Cl_2.

the 5′-*O*-DMT-derivative **10** under standard conditions. Phosphitylation of **10** in anhydrous CH_2Cl_2 in the presence of $^{i}Pr_2EtN$ with 2-cyanoethyl-*N*,*N*-diisopropylchlorophosphoramidite furnished the phosphoramidite **11** (Scheme 2).

Also a new phosphoramidite of 7-deaza-2′-deoxyguanosine (**4**) was prepared which does not show drawbacks of the corresponding phosphoramidite used nowadays. This building block is significantly more stable against oxidation and allows normal oxidation conditions in solid-phase oligonucleotide synthesis. The sensitivity of **4** is reduced by the protection of the 6-oxo group of compound **12** with a diphenylcarbamoyl residue generating a fully aromatic nucleobase. For this purpose nucleoside **12** was treated with diphenylcarbamoyl chloride in pyridine to yield the 6-oxo-protected nucleoside **13**. Phosphitylation with 2-cyanoethyl-*N*,*N*-diisopropylchlorophosphoramidite furnished phosphoramidite **14** (Scheme 3).

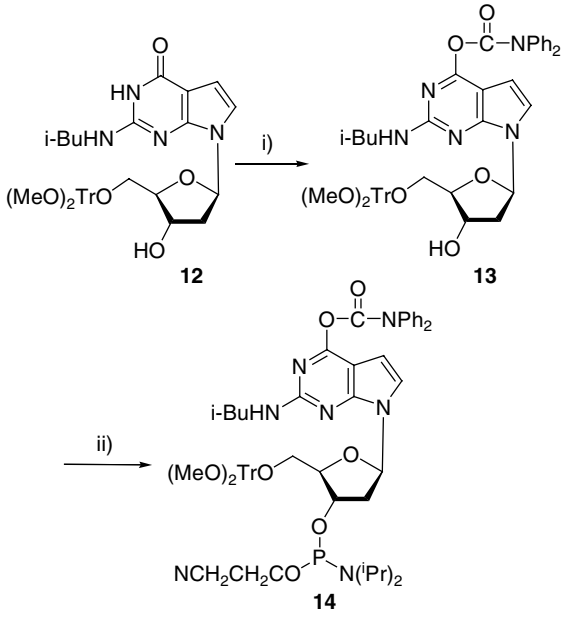

Scheme 3. Synthesis of compound **14**. Reagents: (i) diphenylcarbamoyl chloride, anhydrous pyridine, *N*,*N*-diisopropylethylamine; (ii) 2-cyanoethyl-*N*,*N*-diisopropylchlorophosphoramidite, *N*,*N*-diisopropylethylamine, CH_2Cl_2.

All new monomers were characterized by elemental analyses as well as by ^{1}H and ^{13}C NMR spectra (Table 1).

2.2. Sequence selection and duplex stability in the presence or absence of dyes

Earlier studies using natural DNA with heterogeneous base sequences have shown that actinomycin D binding strength is directly correlated to the dG–dC content of duplex DNA. Crystal structures of the actinomycin D complex showed that the binding is intercalative and the phenoxazone moiety is inserted between two dG–dC base pairs. These studies were extended to short aps duplexes with defined sequence. It was observed that neighbors next to the dG–dC base pairs influence binding. Moreover, it was found that binding occurs between other base pair motifs in which the intercalated drug has only one dG–dC base pair as nearest neighbor.[33] As we want to be flexible in the replacements of nucleobases around the bound phenoxazone moiety, we selected the duplex 5′-d(G-T)$_6$ (**15**) · 3′-d(C-A)$_6$ (**16**) as a reference for duplexes with anti-parallel chain orientation and the duplexes 5′-d(G-T)$_6$ (**15**) · 5′-d(**6**-A)$_6$(**19**) and 5′-d(**7**-T)$_6$ (**20**) · 5′-d(C-A)$_6$ (**21**) as those with parallel chains. Oligonucleotide duplexes are shown in Table 2.

The aps-duplex **15** · **16** with a T_m value of 56 °C contains six dG–dC pairs (motif Ia, Fig. 1) and six dA–dT base pairs. This duplex is designed as a target molecule for actinomycin D or actinomin binding to aps-DNA. Within this duplex the dG residues can be replaced by 7-deaza-2′-deoxyguanosine (**4**, c^7G_d) (motif Ib, duplex **17** · **16**) and 2-amino-7-deazapurine 2′-deoxyribofuranoside (**5**) (duplex **18** · **18**). In order to study the binding selectivity on duplexes with parallel chain orientation, the dG–dC pairs (motif Ia) of the duplex **15** · **16** were replaced by dG–iC_d pairs (motif III, duplex **15** · **19**) or iG_d–dC pairs (motif IV, duplex **20** · **21**). Also base pairs **7**:**6** (motif II, aps duplex **20** · **25**) and **8a–c**: dC (motif V, ps duplexes **22** · **21**, **23** · **21**, and **24** · **21**) are introduced in the oligonucleotides. These base pair motifs are shown in Figure 1.

The T_m values of all duplexes without ligands and in the presence of ligands are shown in Table 2. From that it is apparent that ps duplexes are less stable than those with

Table 1. ^{13}C NMR Chemical shifts (δ) of 7-deazapurine nucleosides[a]

Compound[b,c]	C(2)[d] C(2)	C(4)[d] C(6)	C(4a) C(5)	C(5) C(7)	C(6) C(8)	C(7a)[d] C(4)	C(1′)	C(2′)	C(3′)	C(4′)	C(5′)
5	159.6	150.3	111.1	100.0	122.1	152.6	81.7	39.7	70.6	87.2	61.7
9	152.4	150.6	101.1	116.0	126.1	151.3	82.3	[e]	71.1	87.3	61.9
10	152.3	150.6	101.0	116.0	126.0	151.1	82.4	[e]	70.7	85.4	64.2
12[f]	146.7	156.5	104.2	102.7	119.0	147.5	82.5	[e]	70.6	85.3	64.0
13	141.7	157.0	105.5	99.5	125.8	144.9	82.9	[e]	70.8	85.5	64.3

[a] Measured in DMSO-d_6.
[b] Systematic numbering.
[c] Purine numbering.
[d] Tentative.
[e] Superimposed by DMSO.
[f] See Ref. 32.

Table 2. T_m-Values of duplexes in the presence and the absence of actinomycin (**1**) and actinomin (**2**)[a,b]

Duplex		T_m (°C)		
		Without dye	With actinomycin	With actinomin
5′-d(G-T-G-T-G-T-G-T-G-T-G-T)	(**15**)	56	58	58
3′-d(C-A-C-A-C-A-C-A-C-A-C-A)	(**16**)			
5′-d(**4**-T-**4**-T-**4**-T-**4**-T-**4**-T-**4**-T)	(**17**)	56	59	58
3′-d(C-A-C-A-C-A-C-A-C-A-C-A)	(**16**)			
5′-d(A-T-A-C-**5**-T-A-C-**5**-T-A-T)	(**18**)	22	25	22
3′-d(T-A-T-**5**-C-A-T-**5**-C-A-T-A)	(**18**)			
5′-d(**7**-T-**7**-T-**7**-T-**7**-T-**7**-T-**7**-T)	(**20**)	63	63	66
3′-d(**6**-A-**6**-A-**6**-A-**6**-A-**6**-A-**6**-A)	(**25**)			
5′-d(G-T-G-T-G-T-G-T-G-T-G-T)	(**15**)	40	40	41
5′-d(**6**-A-**6**-A-**6**-A-**6**-A-**6**-A-**6**-A)	(**19**)			
5′-d(**7**-T-**7**-T-**7**-T-**7**-T-**7**-T-**7**-T)	(**20**)	46	46	47
5′-d(C-A-C-A-C-A-C-A-C-A-C-A)	(**21**)			
5′-d(**8a**-T-**8a**-T-**8a**-T-**8a**-T-**8a**-T-**8a**-T)	(**22**)	46	46	47
5′-d(C-A-C-A-C-A-C-A-C-A-C-A)	(**21**)			
5′-d(**8b**-T-**8b**-T-**8b**-T-**8b**-T-**8b**-T-**8b**-T)	(**23**)	61	61	62
5′-d(C-A-C-A-C-A-C-A-C-A-C-A)	(**21**)			
5′-d(**8c**-T-**8c**-T-**8c**-T-**8c**-T-**8c**-T-**8c**-T)	(**24**)	58	58	60
5′-d(C-A-C-A-C-A-C-A-C-A-C-A)	(**21**)			

[a] Measurements were performed in 100 mM NaCl, 10 mM $MgCl_2$, 10 mM sodium cacodylate, pH 7.0. Melting temperatures (T_m-values) were taken from the first derivative of the melting curve (A_{260} vs temperature) measured from 20 to 80 °C with 1 °C min^{-1} temperature increase.
[b] The concentration of oligonucleotide duplexes and of actinomycin or actinomin was 5.0 μM (1:1 ratio).

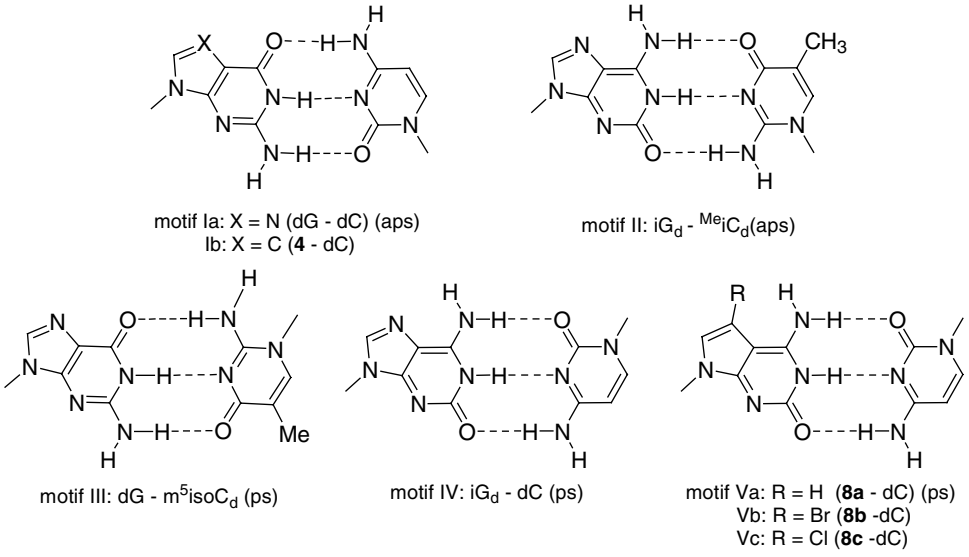

Figure 1. Base pair motifs of ps or aps duplexes containing canonical and modified nucleosides.

aps chain orientation, except for those incorporating the 7-halogenated 7-deaza-2′-deoxyisoguanosines which show a higher stability than that of the reference duplex **15** · **16**. The latter indicates that the halogen substituents increase duplex stability most likely by better base stacking and shows that the halogeno substituents are well accommodated in the groove of parallel DNA.[34] From Table 2 it is obvious that the addition of the actinomycin D increases the melting temperature of aps duplexes containing dG–dC (duplex **15** · **16**) or c^7G_d–dC base pairs (duplex **17** · **16**) or those incorporating 2-amino-7-deazapurine residues (duplex **18** · **18**) by about 2–3 °C. A typical melting profile of the aps duplex **17** · **16** in the presence and absence of actinomycin D is shown in Figure 2, which indicates that the melting temperature of the aps duplex incorporating c^7G_d–dC base pairs was increased by about 3 °C after the addition of the actinomycin D. The aps duplex containing iG:iC base pairs (**20** · **25**) as well as ps duplexes do not show such an increase. This clearly demonstrates that actinomycin D can bind to aps DNA containing dG residues or its 7-deaza analogs or those incorporating 2-amino-7-deazapurines, but not to those incorporating iGd:iCd base pairs. It shows weak bind to ps DNA containing dG-iCd base pairs but no binding to those incorporating iGd-dC base pairs.

Different from actinomycin D its analog **2** is bound both to aps and ps duplexes thereby increasing the T_m values by 1–3 °C (Table 2). In the case of self-complementary

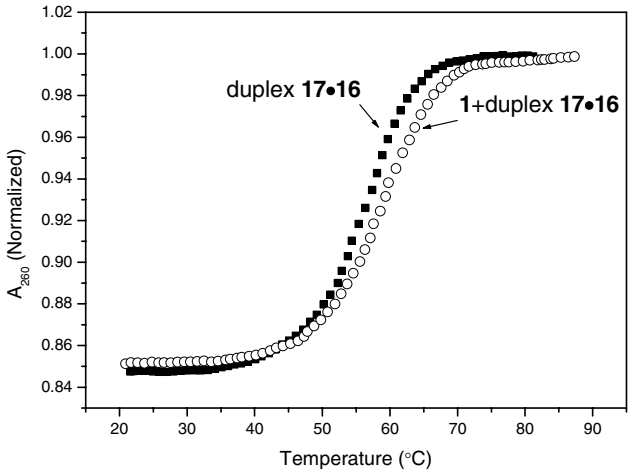

Figure 2. Normalized absorbance-temperature profiles of DNA melting of the duplex **17** · **16** in the absence of actinomycin (squares) and in the presence of compound **1** (1:1 ratio) (circles). For details see Section 4.

aps duplex **18** · **18** containing four nucleoside **5**-residues, the T_m-increase was not observed in the presence of actinomin, a phenomenon which will be discussed below.

2.3. CD spectra

The binding of compounds **1** and **2** to duplex DNA was also monitored by comparing the CD spectra of the drug and the drug/duplex complex. As shown in Figure 3a, the aps-DNA (**15** · **16**) adopts the spectrum of a typical B-type structure. The maxima of positive and negative lobes are located at 278 and 240 nm. The molar ellipticities of these two bands are increased by the addition of compound **1** or **2**. Furthermore, the CD maxima of drug–DNA complexes are shifted to longer wavelength compared to the original spectra. Similar observations are made when compound **2** was bound to other duplexes, while in the case of compound **1**, such phenomenon can only be observed with aps duplexes containing dG:dC or c^7G_d:dC base pairs (**15** · **16** or **17** · **16**). For example, for the ps duplex **20** · **21**, the CD spectra did not change after the addition of compound **1** (Fig. 3b), while the addition of compound **2** leads to strong spectral changes, especially at 260 nm. Thus, the high affinity of compound **2** to aps and ps duplexes as well as that of compound **1** to aps duplexes is verified.

2.4. Fluorescent dye intercalator displacement

Fluorescence intercalator displacement (FID) is a technique for establishing the DNA binding affinity, sequence selectivity, and binding stoichiometry. The method was introduced by Boger[30] and was reviewed recently.[35] Currently, this protocol was applied for the analyses of DNA-binding by peptide derived natural products.[36] In the work described next, a fluorescent intercalator displacement assay (FID) was performed on complementary oligonucleotide duplexes. They were treated with ethidium bromide (**3**), resulting in a fluorescence increase upon binding. It was expected that the bound intercalator **3** can be displaced when the duplex shows stronger binding toward other ligands (**1** or **2**), thereby leading to a decrease of the fluorescence of compound **3**. The extent of fluorescence decrease should be directly related to the binding ability of compound **1** or **2**. Typical results are shown in Figure 4. In the aps duplex **15** · **16**, the fluorescence intensity of compound **3** is decreased due to the addition of compound **1** or **2**, resulting from the release of the bound **3**. It can be deduced that the complexes formed between aps duplexes **15** · **16** and compound **1** or **2** are more stable than that with ethidium bromide **3**. For the ps duplex **20** · **21** the situation is different. The formation of the actinomin–DNA complex was observed accompanied by a decreasing fluorescence of **3** (Fig. 4b). As the fluorescence decrease was almost identical in both cases (Fig. 4b), the binding constant of actinomin (**2**) to the ps duplex **20** · **21** is similar to that of aps-DNA (**15** · **16**). However, when compound **1** was added to a mixture of the ps duplex **20** · **21** and compound **3** the fluorescence changed only very little. The results observed by the FID assays are consistent with the former T_m and CD-measurements.

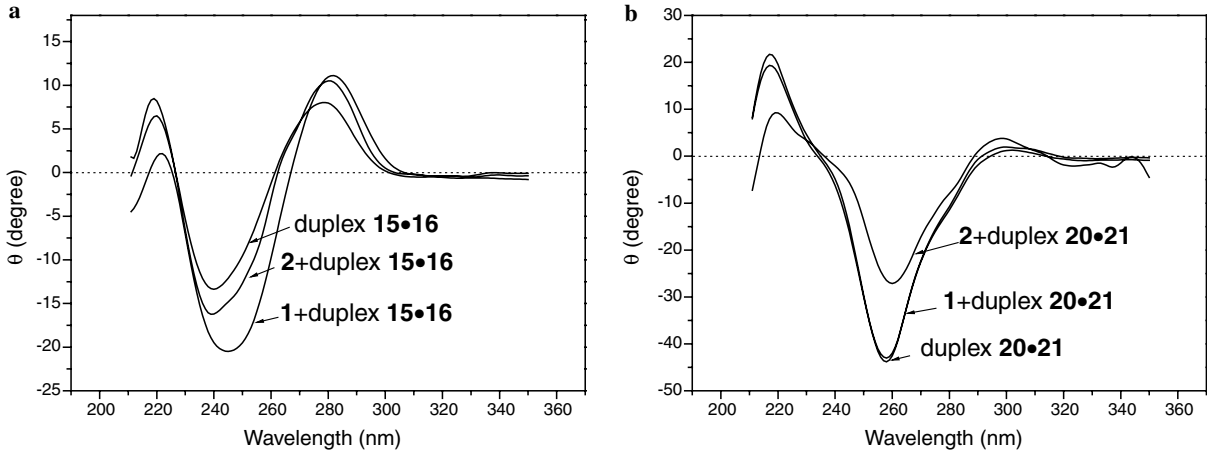

Figure 3. (a) CD spectra of the aps duplex **15** · **16** and in the presence of compounds **1** or **2** (1:1 ratio); (b) CD spectra of the ps duplex **20** · **21** and in the presence of compounds **1** or **2** (1:1 ratio). For details see Section 4.

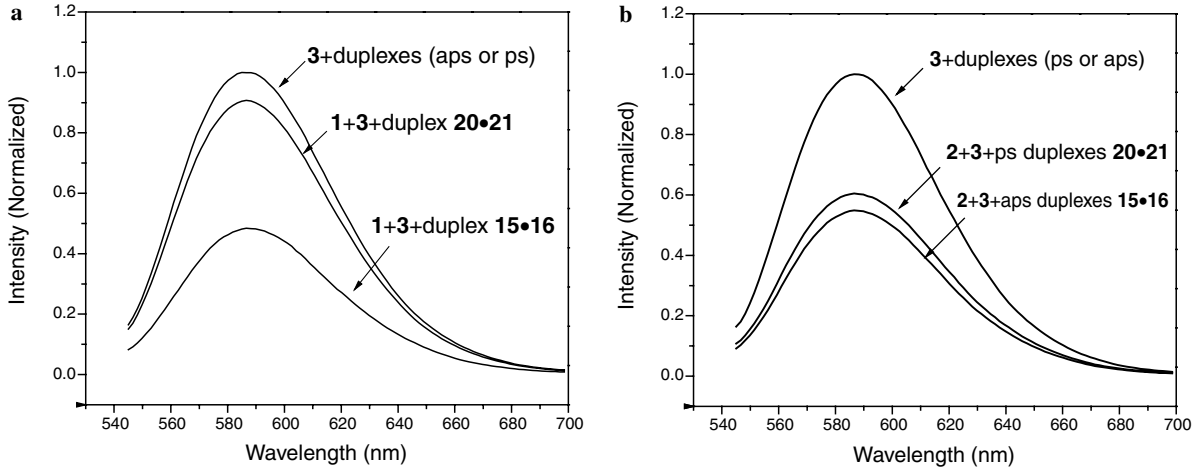

Figure 4. Fluorescence emission spectra of ethidium bromide (**3**) bound to the duplexes **20** · **21** or **15** · **16** (a) in the presence and absence of actinomycin D (**1**) and (b) of actinomin (**2**). The excitation wavelength is 527 nm. Conditions see Section 4.

2.5. Determination of binding constants of compounds 1 and 2 to duplexes with parallel and anti-parallel chain orientation

Figure 5 shows the absorption spectral changes of compound **1** or **2** by the addition of the duplexes selected from Table 2 (for details, see Section 4). With the titration of the aps duplex 5′-d(G-T)$_6$ (**15**) · 3′-d(C-A)$_6$ (**16**) both dyes generate a bathochromic shift of the visible spectra with a hypochromic change, which is consistent with earlier findings on high molecular DNA (Figs. 5a and b).[9] This results from the intercalation of the phen-

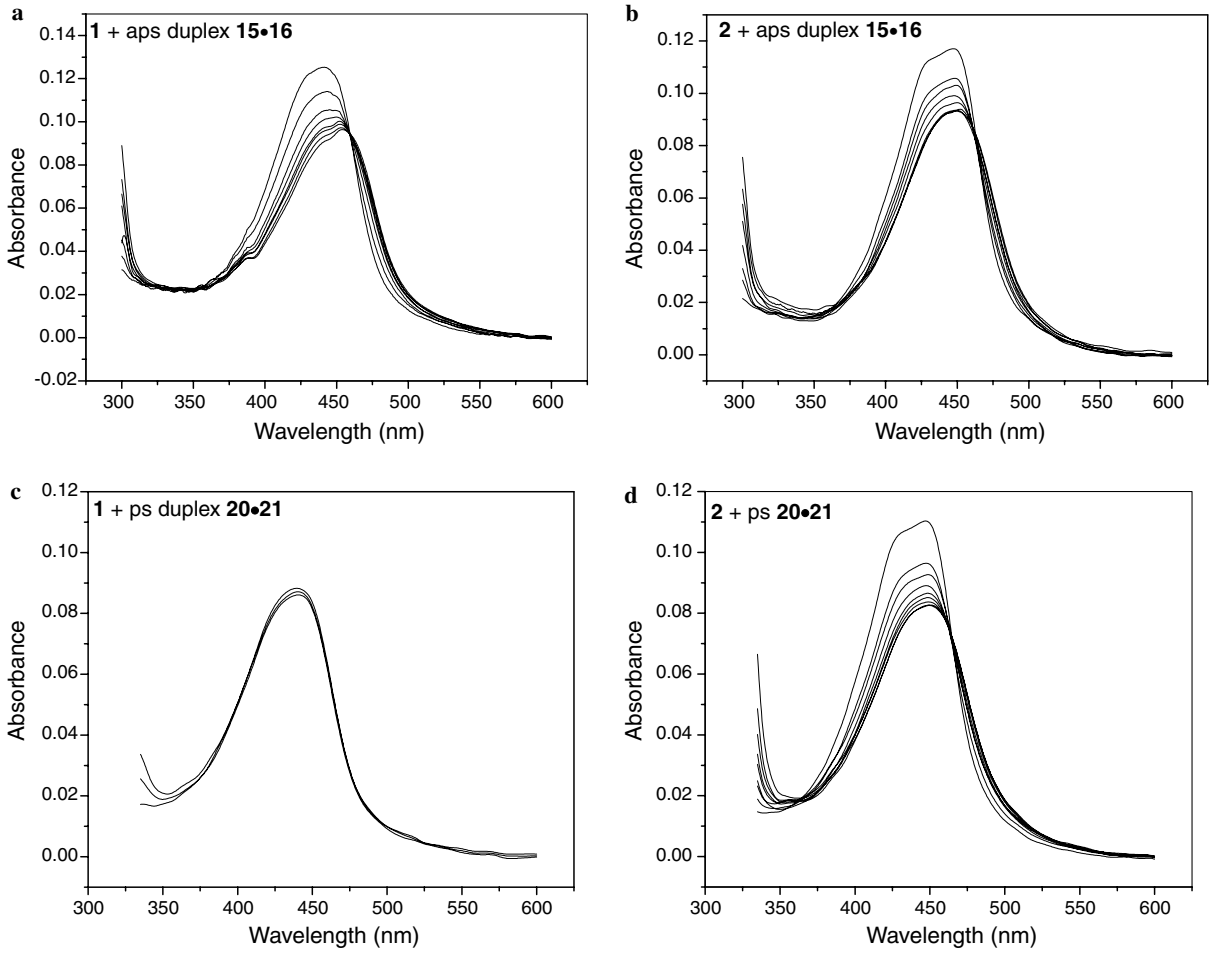

Figure 5. Visible absorption spectral changes after the addition of duplexes **15** · **16** and **20** · **21** to compounds **1** (a,c) and **2** (b,d). Conditions see Section 4.

oxazone moiety into the DNA duplex.[33] It was already proven long ago with actinomycin D derivatives carrying bulky *t*-butyl groups instead of the canonical methyl substituents in the 4- and 6-positions of the chromophore that intercalation in duplex DNA cannot occur.[25,37] The titration curves show an isosbestic point at 458 nm for compound **1** and at 464 nm for compound **2** (Figs. 5a and b). These significant changes are indicative of intercalation. Similar changes of the absorption spectra of compound **1** or **2** are observed when dG was displaced by compound **4** or **5** to form the aps duplex **17 · 16** or **18 · 18**. However, the titration of the aps duplex **20 · 25** containing $isoG_d$–$isoC_d$ base pairs leads to the change of the absorption spectra of actinomin (**2**), while no change is observed for that of actinomycin D.

When ps duplexes (**20 · 21**, **22 · 21**, and **23 · 21**) were added to the solution of compound **1**, respectively, the absorption spectra always kept the same (Fig. 5c). Only the ps duplex **15 · 19**, which is composed of dG:$isoC_d$ and dA:dT base pairs shows a bathochromic shift with only a small hypochromic change (data not shown). The weak binding of compound **1** to the ps duplex **15 · 19** was not detected by T_m and CD measurements probably for sensitivity reasons. The titration experiments performed with actinomin (**2**) and ps duplexes result in a totally different behavior. No matter which ps duplex was used, the absorption spectra of the dye changed in a way typical for phenoxazone intercalation (for spectra, see Fig. 5d).

To obtain quantitative binding parameters, the titration data were collected at fixed wavelengths (440 nm for compound **1** and 443 nm for compound **2**) and were plotted in a Scatchard graph as shown in Figure 6. The linear region of the binding isotherm at small *r* values (*r* equals bound drug molecules per duplex) was fitted to Eq. (2). The slope of the line gives the apparent binding constant ($-K_{ap}$) and the intercept on the *x*-axis results in the multiply of the apparent number of binding sites per duplex (B_{ap}) and the binding constant. The observed equilibrium constants and the number of binding sites per duplex (B_{ap}) are listed in Table 3. With the aps duplex **15 · 16** compound **1** shows the highest binding constant, $K = 2.1 \times 10^6\ M^{-1}$; the number of binding sites per duplex is 0.9 (one binding site out of 14 base pairs). These data are in agreement with previously reported values for compound **1** with poly d(T-G) · poly d(C-A) ($K = 2 \pm 1 \times 10^6\ M^{-1}$ with one binding site out of 18 ± 8 base pairs).[33] The substitution of the dG residues by the 7-deazapurine nucleoside **4** (duplex **17 · 16**) or **5** (duplex **18 · 18**) reduces the binding constant but still keeping them in the similar range (Table 3). As already mentioned above, the ps duplex **15 · 19** showed a weak binding to compound **1** (see Table 3).

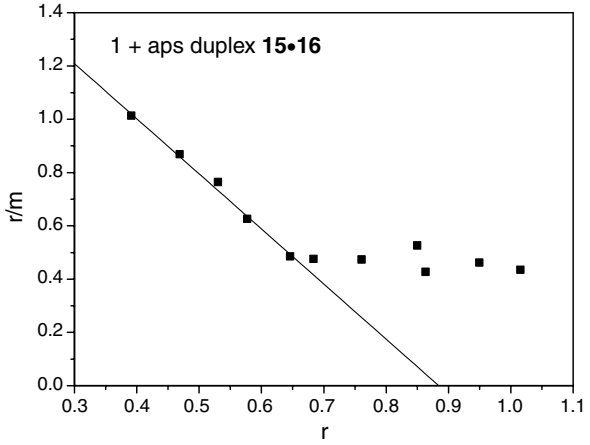

Figure 6. Typical binding isotherm of compound **1** to the aps duplex **15 · 16** at 20 °C. The solid line results from a linear least-squares fit using the Scatchard equation $r/m = K_{ap}(B_{ap} - r)$, where *r* is the value of bound dye per mole of duplex; *m* is the concentration of free drug; B_{ap} is the apparent number of binding sites per mole of duplex and K_{ap} is the apparent binding constant.

Table 3. Comparison of the apparent binding constants of compound **1** or **2** to aps and ps duplexes

Chain orientation	Duplex	K_{ap} (M^{-1})		B_{ap}[a]	
		1	**2**	**1**	**2**
Anti-parallel	**15 · 16**	2.1×10^6	2.0×10^6	0.9	3.0
	17 · 16	1.3×10^6	0.8×10^6	1.0	2.0
	18 · 18	0.4×10^6	n.b.[b]	1.5	n.b.[b]
	20 · 25	n.b.	1.5×10^6	n.b.[b]	2.0
Parallel	**15 · 19**	$\ll 0.1 \times 10^6$	0.4×10^6	n.d[c]	2.0
	20 · 21	n.b.	1.9×10^6	n.b.[b]	2.4
	22 · 21	n.b.	0.7×10^6	n.b.[b]	2.0

[a] B_{ap}, number of binding sites per duplex.
[b] n.b., no binding.
[c] n.d., not determined.

The situation is different for the binding properties of actinomin (**2**). This molecule displays high affinities to aps and ps duplexes containing dG:dC base pairs or analogs thereof. The exemption found for the duplex **18 · 18** is probably due to its low thermal stability. The binding constants of **2** are always in the range from 10^5 to $10^6\ M^{-1}$ and the binding sites are about two per duplex which is significantly higher than that for actinomycin D.

2.6. Discussion

The requirement of guanine residues for actinomycin D (**1**) binding is well established for duplexes with anti-parallel chain orientation.[9,15] This results from a hydrogen bond existing between the 2-amino group of the guanine moiety and the carbonyl oxo group of the L-threonine residue; a second hydrogen bond is formed between the nitrogen-3 of the guanine ring (as an acceptor) and the proton of the amide function of the L-threonine moiety (as a donor).[13] During complex formation the phenoxazone moiety of **1** is inserted into the DNA duplex between two dG–dC base pairs. But as reported earlier one dG–dC base pair next to actinomycin is sufficient to bind the antibiotic.[33] This is consistent with our observation that the aps duplex $d(G\text{-}T)_6 \cdot d(C\text{-}A)_6$ shows strong binding to compound **1**. The formation of drug–DNA complexes was verified by the increase (1–3 °C) of

T_m values of the respective duplexes and the change of their CD spectra. Due to the high affinity of compound **1** to aps duplexes such as **15** · **16**, a fluorescent dye intercalator displacement assay with pre-bound ethidium bromide (**3**) was performed. Replacement of ethidium bromide by the drug resulted in a strong fluorescence decrease. The same protocols were applied to the duplexes containing modified nucleosides. The binding of compound **1** was found to be rather strong when the dG-residues were replaced by the 7-deazapurine analogs **4** or **5**, while the aps duplexes containing $isoG_d$–$isoC_d$ base pairs do not bind actinomycin D due to the absence of the 2-amino group.

The binding behavior of compound **1** to the corresponding duplexes with parallel chain orientation is different. Duplexes with $isoG_d$–dC base pairs do not bind actinomycin D, while in ps duplexes containing dG-$isoC_d$ such as **15** · **19** the binding is detectable but weak. This shows that the dG-residues present in ps duplexes can form hydrogen bonds with compound **1**. The reduced affinity of actinomycin D to the ps duplex **15** · **19** is likely caused by steric restrictions of the groove size of ps-DNA which has to accommodate the peptide lacton rings of the antibiotic molecule. In aps-DNA, the shape of the chiral peptide lacton ring follows the spatial requirements of the minor groove of B-DNA. This chiral recognition has already been studied with an enantiomeric analog of actinomycin D which does not bind to aps-DNA.[38] In all binding processes, solvent molecules, associated to the backbone of DNA or the peptide lacton rings, have to be reorganized. It has been shown that the minor groove becomes shallow and wide when the chain orientation changes from anti-parallel to parallel, the groove of ps duplexes cannot well accommodate the peptide rings of compound **1**. The binding of actinomin (**2**) to duplex DNA is not strongly related to the chain orientation. As shown in Scheme 1, compound **2** has the same phenoxazone chromophore as compound **1** but different side chains. The positively charged triethylamino groups of **2** can interact with the negative charges of the phosphodiester backbone electrostatically forming interactions which are obviously similar both in ps- and aps-DNA.

3. Conclusions

From the work described above the following conclusion can be drawn:

(i) Parallel duplexes containing dG-$isoC_d$ base pairs bind actinomycin but with a much lower affinity than anti-parallel duplexes with dG–dC pairs. This indicates that the interaction of ps-DNA is strongly controlled by chiral recognition of the peptide lacton rings and the grooves of DNA.
(ii) Actinomycin binds to aps-DNA when 2′-deoxyguanosine is replaced by 7-deaza-2′-deoxyguanosine **4** or its 6-deoxo derivative **5**. Novel phosphoramidites of **4** and **5** were prepared. The new building block of **4** does not show drawbacks of the corresponding phosphoramidite used nowadays. This building block is significantly more stable against oxidation and allows normal oxidation conditions in solid-phase oligonucleotide synthesis.
(iii) Anti-parallel oligonucleotide duplexes containing $isoG_d$–$isoC_d$ base pairs or parallel duplexes containing base pairs of $isoG_d$–dC do not bind actinomycin due to the absence of the guanine 2-amino group.
(iv) Actinomin binds to parallel as well to anti-parallel DNA. It is not only bound to DNA with canonical base pairs but shows strong binding to duplexes incorporating modified dG- or iG_d-residues, for example, 7-deazapurines instead of purines. Bulky 7-halogen substituents which were present in ps duplexes do not impair actinomin binding.

4. Experimental

4.1. Synthesis of compounds 9–14

4.1.1. General. All solvents are of laboratory grade. Other chemicals were bought from Sigma-Aldrich Chemie GmbH (Deisenhofen, Germany). Compound **2** was prepared according to Seela.[25] The synthesis of compounds **4**–**8** is described earlier.[31,39–43] The phosphoramidites of compounds **6**, **7**, and **8a**–**c** were synthesized as described.[34,43,44] The standard phosphoramidites are commercial materials bought from Proligo (Hamburg, Germany). Thin-layer chromatography (TLC) was performed on TLC aluminum sheets covered with silica gel 60 F_{254} (0.2 mm, VWR International, Darmstadt, Germany). Column flash chromatography (FC) was accomplished on silica gel 60 (VWR International, Darmstadt, Germany) at 0.4 bar. NMR spectra were measured on an Avance-250 or AMX-500 spectrometer (Bruker, Rheinstetten, Germany); Chemical shifts (δ) are in ppm relative to internal Me_4Si or external H_3PO_4 (^{31}P). The J values are given in Hz. Elemental analyses were performed by the Mikroanalytisches Laboratorium Beller, Göttingen, Germany.

4.1.2. 7-(2-Deoxy-β-D-*erythro*-pentofuranosyl)-2-formylamino-7*H*- pyrrolo[2,3-*d*]pyrimidine (9). Into a solution of 7-(2-deoxy-β-D-*erythro*-pentofuranosyl)-7*H*-pyrrolo-[2,3-*d*]pyrimidin-2-amine[31] (**5**: 750 mg, 3.0 mmol) in MeOH (40 mL), dimethylformamide dimethylacetal (6.0 mL, 44.8 mmol) was added and the mixture was stirred at 50 °C for 24 h. After removal of the solvent, the residue was redissolved in MeOH (40 mL) and two drops of water were added. The solution was stirred at 30–40 °C for 72 h and adsorbed on a small amount (5.0 g) of silica gel. This material was loaded on the top of a silica gel column (4× 15 cm), and the product was eluted stepwise with CH_2Cl_2/MeOH (98:2, 300 mL) and CH_2Cl_2/MeOH (95:5, 600 mL). The product-containing fractions were combined and evaporated to give a colorless foam (550 mg, 66%); TLC (CH_2Cl_2/MeOH 9:1): R_f 0.32; UV (MeOH): λ_{max} 238 (19,800), 274 (4460), 303 (2800); ^1H NMR (DMSO-d_6): δ 2.16–2.25 (m, 1H, 2′-H), 2.50–2.56 (m, 1H, 2′-H), 3.47–3.82 (m, 2H, 5′-H), 3.81–3.83 (m, 1H, 4′-H), 4.35–4.37 (m, 1H, 3′-H), 4.90 (t, J = 5.3 Hz, 1H, 5′-OH), 5.30 (d, J = 3.8 Hz, 1H, 3′-OH), 6.54–6.62 (m, 2H, 5-H, 1′-H),

7.65 (d, J = 3.7 Hz, 1H, 6-H), 8.80 (s, 1H, 4-H), 9.43 (d, J = 9.8 Hz, 1H, NH), 10.82 (d, J = 9.8 Hz, 1H, COH); Anal. Calcd for $C_{12}H_{14}N_4O_4$ (278.26): C 51.80, H 5.07, N 20.13; found: C 51.70, H 4.97, N 20.15.

4.1.3. 7-[2-Deoxy-5-*O*-(4,4′-dimethoxytriphenylmethyl)-β-D-*erythro*-pentofuranosyl]-2-formylamino-7*H*-pyrrolo[2,3-*d*]pyrimidine (10). Compound **9** (355 mg, 1.28 mmol) was co-evaporated three times with anhydrous pyridine (3 mL each) and dissolved in anhydrous pyridine (6.0 mL). Into this solution, 4,4′-dimethoxytriphenylmethyl chloride (517 mg, 1.53 mmol) was added and stirred at rt for 6 h. The reaction mixture was quenched by the addition of MeOH (1 mL) and evaporated to dryness. The residue was dissolved in CH_2Cl_2 (30.0 mL) and washed twice with 5% aq $NaHCO_3$ (15 mL) and once with brine (15 mL). The organic layer was dried over anhydrous Na_2SO_4, filtered, and evaporated to dryness. The crude product was redissolved in CH_2Cl_2 (2.0 mL) and submitted to FC (column 4× 10 cm, elution with CH_2Cl_2/MeOH, 98:2), yielding a colorless foam (550 mg, 74%); TLC (CH_2Cl_2/MeOH, 95:5): R_f 0.26; UV (MeOH): λ_{max} 243 (59,000), 276 (14,225), 300 (12,770); ^{1}H NMR (DMSO-d_6): δ 2.26–2.31 (m, 1H, 2′-H), 2.58–2.65 (m, 1H, 2′-H), 3.15–3.21 (m, 2H, 5′-H), 3.72 (s, 6H, 2MeO), 3.92–3.94 (m, 1H, 4′-H), 4.38–4.41 (m, 1H, 3′-H), 5.35 (d, J = 3.9 Hz, 1H, 3′-OH), 6.54–6.59 (m, 2H, 1′-H, 5-H), 6.78–6.83 (m, 4H, arom. H), 7.19–7.36 (m, 9H, arom. H), 7.47 (d, J = 2.9 Hz, 1H, 6-H), 8.81 (s, 1H, 4-H), 9.41 (d, J = 10.3 Hz, 1H, NH), 10.81 (d, J = 10.3 Hz, 1H, COH); Anal. Calcd for $C_{33}H_{32}N_4O_6$ (580.6): C 68.26, H 5.56, N 9.65; found: C 68.18, H 5.60, N, 9.56.

4.1.4. 7-[2-Deoxy-5-*O*-(4,4′-dimethoxytriphenylmethyl)-β-D-*erythro*-pentofuranosyl]-2-formylamino-7*H*-pyrrolo[2,3-*d*]pyrimidine 3′-(2-cyanoethyl)-*N*,*N*-diisopropylphosphoramidite (11). Into a solution of compound **10** (200 mg, 0.34 mmol) in anhydrous CH_2Cl_2 (3.0 mL), *N*,*N*-diisopropylethylamine (DIPEA) (0.1 mL, 0.57 mmol) and 2-cyanoethyl-*N*,*N*-diisopropylchlorophosphoramidite (0.1 mL, 0.45 mmol) were added under an Ar atmosphere. The reaction mixture was stirred at rt for 30 min, diluted with CH_2Cl_2 (20 mL), and washed twice with 5% aq $NaHCO_3$ (10 mL), followed by brine (10 mL). The organic layer was dried over Na_2SO_4, filtered, evaporated, and the residue was submitted to FC (column 3 × 9 cm, CH_2Cl_2/acetone, 95:5), yielding a colorless foam (207 mg, 77%); TLC (CH_2Cl_2/acetone, 9:1): R_f 0.20, 0.26; ^{1}H NMR ($CDCl_3$): δ 1.11–1.20 (m, 12H, 4Me), 2.46 (t, J = 6.7 Hz, OCH_2CH_2CN), 2.60–2.65 (m, 2H, 2′-H), 3.25–3.39 (m, 2H, Me_2CH), 3.58–3.72 (m, 4H, 5′-H, OCH_2CH_2CN), 3.78 (s, 6H, 2MeO), 4.22–4.24 (m, 1H, 4′-H), 4.68–4.72 (m, 1H, 3′-H), 6.44 (d, J = 3.4 Hz, 1H, 5-H), 6.66 (t, J = 6.6 Hz, 1H, 1′-H), 6.77–6.82 (m, 4H, arom. H), 7.22-7.41 (m, 10H, arom. H, 6-H), 8.19 (d, J = 11.3 Hz, 1H, NH), 8.69 (s, 1H, 4-H), 9.53 (d, J = 11.4 Hz, 1H, COH); ^{31}P NMR ($CDCl_3$): 150.1, 149.9.

4.1.5. 7-[2-Deoxy-5-*O*-(4,4′-dimethoxytriphenylmethyl)-β-D-*erythro*-pentofuranosyl]-3,7-dihydro-2-[(2-methylpropanoyl)amino]-4*H*-pyrrolo[2,3-*d*]pyrimidin-4-yl diphenylcarbamate (13). Compound **12**[32] (3.9 g, 6.1 mmol) was co-evaporated three times with anhydrous pyridine (15 mL each) and dissolved in anhydrous pyridine (30 mL). Then, diphenylcarbamoyl chloride (dpc-Cl) (2.5 g, 10.8 mmol) and *N*,*N*-diisopropylethylamine (DIPEA) (1.5 mL, 8.6 mmol) were added. After stirring at rt for 2 h, the excess of dpc-Cl was destroyed with crushed ice (∼50 mL), the mixture was poured into 5% aq $NaHCO_3$ (50 mL) and extracted with CH_2Cl_2 (3× 100 mL). The combined organic layer was dried over anhydrous Na_2SO_4, filtered, and evaporated. The residue was submitted to FC (column 4 × 15 cm, elution stepwise with CH_2Cl_2 → CH_2Cl_2/acetone 9:1), yields a colorless foam (3.9 g, 77%); TLC (CH_2Cl_2/acetone 9:1): R_f 0.5; ^{1}H NMR (DMSO-d_6): δ 1.06–1.08 (m, 6H, CH_3), 2.25–2.30 (m, 1H, 2′-H), 2.57–2.68 (m, 1H, 2′-H), 2.73–2.81 (m, 1H, C*H*), 3.14–3.25 (m, 2H, 5′-H), 3.69 (s, 6H, OCH_3), 3.93–3.95 (m, 1H, 4′-H), 4.40–4.42 (m, 1H, 3′-H), 5.36 (d, J = 3.4 Hz, 1H, 3′-OH), 6.56 (t, J = 6.7 Hz, 1H, 1′-H), 6.64 (d, J = 2.7 Hz, 1H, 5-H), 6.82 (m, 4H, arom. H), 7.21–7.49 (m, 20H, arom. H, 6-H), 10.54 (s, 1H, N*H*); Anal. Calcd for $C_{49}H_{47}N_5O_8$ (833.93): C 70.57, H 5.68, N 8.40; found: C 70.43, H 5.61, N 8.34.

4.1.6. 7-[2-Deoxy-5-*O*-(4,4′-dimethoxytriphenylmethyl)-β-D-*erythro*-pentofuranosyl]-3,7-dihydro-2-[(2-methylpropanoyl)amino]-4*H*-pyrrolo[2,3-*d*]pyrimidin-4-yl diphenylcarbamate 3′-(2-cyanoethyl *N*,*N*-diisopropylphosphoramidite) (14). To a solution of **13** (1.0 g, 1.2 mmol) in anhydrous CH_2Cl_2 (15 mL), *N*,*N*-diisopropylethylamine (0.6 mL, 3.4 mmol) and 2-cyanoethyl diisopropylphosphoramidochloridite (0.6 mL, 2.7 mmol) was added. The mixture was stirred at rt for 15 min, diluted with CH_2Cl_2 (50 mL) and washed twice with 5% aq $NaHCO_3$ (50 mL), followed by brine (30 mL). The organic layer was separated and the aqueous layer was extracted twice with CH_2Cl_2 (20 mL each). The combined organic layers were dried over anhydrous Na_2SO_4, filtered and evaporated. The oily residue was applied to FC (column 4 × 10 cm, CH_2Cl_2 → CH_2Cl_2/acetone 95:5), yielding a colorless foam (930 mg, 75%); TLC (CH_2Cl_2/acetone 95:5): R_f 0.7; ^{1}H NMR ($CDCl_3$): δ 0.85–1.25 (m, 18H, $6CH_3$), 2.43 (t, J = 6.3 Hz, OCH_2CH_2CN), 2.58–2.67 (m, 2H, 2′-H), 3.26–3.45 (m, 3H, Me_2CH), 3.58–3.72 (m, 4H, 5′-H, OCH_2CH_2CN), 3.77 (s, 6H, 2MeO), 4.18–4.20 (m, 1H, 4′-H), 4.68–4.70 (m, 1H, 3′-H), 6.36 (d, J = 3.4 Hz, 1H, 5-H), 6.63 (t, J = 6.5 Hz, 1H, 1′-H), 6.77–6.82 (m, 4H, arom. H), 7.22–7.39 (m, 10H, arom. H, 6-H), 7.82, 7.87 (2s, 1H, NH); ^{31}P NMR ($CDCl_3$): 150.0, 149.6.

4.2. Oligonucleotide synthesis and purification

The synthesis of the oligonucleotides using the protocol of phosphoramidite chemistry was performed on an ABI 392-08 synthesizer (Applied Biosystems, Weiterstadt, Germany) employing the standard conditions at 1 μmol scale following the synthesis protocol for 3′-cyanoethylphosphoramidites.[45] After cleavage from the solid support, the oligonucleotides were deprotected in 25% aqueous ammonia solution for 12–16 h at 60 °C. Purification of the 5′-dimethoxytrityl oligomers was carried out on a 4 × 250 mm RP-18 (5 μm)

LiChrosorb column (VWR International, Darmstadt, Germany) with a Merck-Hitachi HPLC pump (model 655A-12) connected with a variable wavelength monitor (model 655-A) and a controller (model D-2000). The trityl-on oligomers were chromatographed with the following solvent gradient system [A: 0.1 M (Et_3NH)OAc (pH 7.0)/MeCN 95:5; B: MeCN]: 0–3 min, 10–15% B in A, 3–15 min, 15–50% B in A, 15–20 min, 50–10% B in A, 20–25 min, 10% B in A, the flow rate always being 1.0 mL/min. The solution was dried and treated with 2.5% $CHCl_2COOH/CH_2Cl_2$ for 5 min at room temperature (rt) to remove the 4,4′-dimethoxytrityl residue. The detritylated oligomers were purified by reversed-phase HPLC with the gradient: 0–25 min, 0–20% B in A with a flow rate of 1.0 mL/min. The oligomers were desalted with a 4×125 mm RP-18 (5 μm) LiChrosorb column (VWR International, Darmstadt, Germany) and lyophilized on a Speed-Vac evaporator to yield colorless solids. The molecular masses of the oligonucleotides were determined by MALDI-TOF mass spectrometry (Table 4). The MALDI-TOF mass spectra were recorded on a Biflex-III spectrometer (Bruker, Leipzig, Germany) in the reflector mode. The average power of the nitrogen laser (337.1 nm) at 20 Hz was 3–4 mW (150–200 μJ/pulse) with a delay time of 600 ns. 3-HPA (3-hydroxypicolinic acid) was used as the matrix. Oligonucleotide concentrations were determined by measuring the absorbance at 260 nm after melting (at 95 °C). The extinction coefficients of the unmodified oligonucleotides were determined according to nearest-neighbor approximation using mono- and di-nucleotide tabulated values.[46] The extinction coefficients at 260 nm of the modified oligonucleotides were calculated from the sum of the extinction coefficients of the monomeric 2′-deoxyribonucleosides corrected by the hypochromicity (Table 4). The hypochromicity ($h = [(\varepsilon_{monomer} - \varepsilon_{polymer}) \times (\varepsilon_{monomer})^{-1}] \times 100\%$) was determined from the absorbance before and after enzymatic digestion with snake-venom phosphodiesterase (EC 3.1.15.1, *Crotallus adamanteus*) (for details see Ref. 34). The hypochromicity was 20% for oligonucleotides **18**, **19**, and **25**, 10% for compounds **17**, **20**, and **22**, and around 5% for **23**, **24** (ε_{260} of monomers: A_d 15,400, C_d 7600, G_d 11,700, T_d 8800, **4** 4300, **5** 4100, **6** 6300, **7** 7600, **8a** 7400, **8b** 5800, and **8c** 6400).

4.3. T_m-measurements

The UV melting of oligonucleotides was performed on a Cary-1/1E UV/VIS spectrophotometer (Varian, Australia) equipped with a Cary thermoelectrical controller. The experiments were carried out by increasing the temperature at a rate of 1 °C/min from 20 to 90 °C and the temperature was recorded every minute. The duplexes were dissolved in buffer solution (100 mM NaCl, 10 mM $MgCl_2$, and 10 mM sodium cacodylate, pH 7.0) using 5.0 μM of single-strand concentration. The T_m values were obtained from the melting curves. Each melting curve was fit to a non-self-complementary two-state model, and the thermodynamic parameters were obtained with the Meltwin 3.0 software package.[47]

4.4. UV Absorption measurement and Scatchard plots

UV spectra were recorded on a U-3200 spectrophotometer (Hitachi, Japan), λ_{max} in nm, ε in $dm^3\ mol^{-1}\ cm^{-1}$. Concentrations of oligonucleotide solutions have been determined using the molar absorption coefficients of the dodecamers (Table 4). Concentrations of the drug solutions were determined by measuring the absorbances at 440 nm (for **1**, ε: 24,500 $M^{-1}\ cm^{-1}$) and 443 nm (for **2**, ε: 26,100 $M^{-1}\ cm^{-1}$).[15,25] Stock solutions for oligonucleotides and drugs were prepared by dissolving the samples in buffer solution (100 mM NaCl, 10 mM $MgCl_2$, and 10 mM sodium cacodylate, pH 7.0).

The titrations were carried out at 20 °C by injecting 2 μL portions of oligonucleotide duplex solutions (duplex concentration, 1.0 μM) to the drug solution having a concentration of 7.5×10^{-6} M. The solutions were thoroughly mixed and equilibrated for 5 min after each addition. The concentration of drug–DNA complex (C_k) was calculated according to the following Eqs. 1 and 2:

$$C_k = (\varepsilon_\lambda^A C_T - A)/(\varepsilon_\lambda^A - \varepsilon_\lambda^k), \quad (1)$$

where ε_λ^A and ε_λ^k are the molar extinction coefficients of free and bound drug, respectively, measured at the wavelength of 440 nm for **1** and 443 nm for **2**, A is the absorbance of the solution, and C_T is the total drug concentration, which was determined by adding 10 μl of the stock solution of **1** or **2** (7.5×10^{-5} M) to a highly

Table 4. Molecular masses $[M+H]^+$ of oligonucleotides determined by MALDI-TOF mass spectrometry and extinction coefficients of oligonucleotides

Oligonucleotide	MH^+ (calcd.)	MH^+ (found)	ε_{260}[a] ($M^{-1}\ cm^{-1}$)	ε_{260}[b] ($M^{-1}\ cm^{-1}$)
5′-d(GTG TGT GTG TGT) (**15**)	3739	3740	123000	98400
5′-d(ACA CAC ACA CAC) (**16**)	3553	3553	138000	110100
5′-d(**4**T**4** T**4**T **4**T**4** T**4**T) (**17**)	3743	3743	78600	70700
5′-d(ATA C**5**T AC**5** TAT) (**18**)	3610	3611	120200	96200
5′-d(**6**A**6** A**6**A **6**A**6** A**6**A) (**19**)	3638	3639	130200	104200
5′-d(**7**T**7** T**7**T **7**T**7** T**7**T) (**20**)	3739	3740	98400	88600
5′-d(CAC ACA CAC ACA) (**21**)	3553	3553	138000	110100
5′-d(**8**a**T8**a**T8**a**T8**a**T8**a**T**) (**22**)	3733	3734	97200	87500
5′-d(**8**b**T8**b**T8**b**T8**b**T8**b**T**)(**23**)	4207	4207	87600	83200
5′-d(**8**c**T8**c**T8**c**T8**c**T8**c**T**) (**24**)	3940	3941	91200	86600
5′-d(A**6**A **6**A**6** A**6**A **6**A**6**) (**25**)	3638	3637	130200	104200

[a] Calculated extinction coefficients.
[b] The extinction coefficients corrected by the hypochromicity.

concentrated DNA (0.1 mM) solution. $\varepsilon_{\lambda}^{k}$ was determined by adding increasing amounts of actinomycin D to a highly concentrated DNA solution. At this high DNA concentration the drug added initially is quantitatively bound, and the extinction coefficient of the complex can be calculated directly.

Binding constants (K) were extracted from linear least-squares fits of the experimental binding isotherms obtained for the binding of **1** or **2** to DNA.

$$A + \mathrm{DNA} = \mathrm{DNA} - \mathrm{A}.$$

The corresponding Scatchard equation used for the analysis of the data is Eq. (2):[48]

$$r/m = K_{\mathrm{ap}}(B_{\mathrm{ap}} - r), \qquad (2)$$

where r is the ratio of bound drug per mole of duplex, m is the concentration of free drug, B_{ap} is the apparent number of binding sites per mole of duplex, and K_{ap} is the apparent binding constant.

4.5. CD spectra

The CD spectra were measured with a Jasco J-600A spectropolarimeter (Jasco, Japan) at room temperature using 1.0 mL water-jacketed cylindrical cells of 1-cm path length. The oligonucleotide samples (5.0 μM single strand concentration) were prepared in the same buffer as used for the T_{m} measurements. The spectra were recorded between 200 nm and 350 nm in intervals of 0.5 nm.

4.6. Fluorescence dye intercalator displacement (FID)

In a quartz cuvette (3.0 mL) containing 1.0 mL buffer solution (100 mM NaCl, 10 mM $MgCl_2$, and 10 mM sodium cacodylate, pH 7.0), ethidium bromide solution (2.0 μl) was added (0.5 mM in buffer solution of 100 mM NaCl, 10 mM $MgCl_2$, and 10 mM sodium cacodylate, pH 7.0). The fluorescence (Hitachi F-4500 spectrophotometer, Hitachi, Japan) was measured and normalized to 0% relative fluorescence. The duplex solution (2.0 μl, 2.0 μM single-strand concentration, 24.0 μM in base pair final concentration) was added, and the fluorescence was measured again and normalized to 100% relative fluorescence. A solution of **1** or **2** (2.0 μl, 7.5×10^{-5} M in buffer solution of 100 mM NaCl, 10 mM $MgCl_2$, 10 mM sodium cacodylate, pH 7.0) was added, and the fluorescence was measured after 3 min of incubation at 20 °C. Subsequent addition of 2.0 μl aliquots was continued until the system reached saturation and the fluorescence remained constant by further compound additions.

Acknowledgments

We thank Dr. Yang He and Ms. Kuiying Xu for the NMR measurements and Prof. Dr. H.-J. Hinz for fruitful discussion. We appreciate the help of Mrs. Monika Dubiel and Mrs. Elisabeth Michalek during the preparation of the manuscript. Financial support by Roche Diagnostics GmbH, Penzberg, is gratefully acknowledged.

Supplementary data

Supplementary data associated with this article can be found, in the online version, at doi:10.1016/j.bmc.2006.02.002.

References and notes

1. Seela, F.; Gabler, B.; Kazimierczuk, Z. *Collect. Czech. Chem. Commun.* **1993**, *58*, 170.
2. Sugiyama, H.; Ikeda, S.; Saito, I. *J. Am. Chem. Soc.* **1996**, *118*, 9994.
3. Seela, F.; Wei, C.; Melenewski, A.; Feiling, E. *Nucleosides Nucleotides* **1998**, *17*, 2045.
4. van de Sande, J. H.; Ramsing, N. B.; Germann, M. W.; Elhorst, W.; Kalisch, B. W.; vonKitzing, E.; Pon, R. T.; Clegg, R. C.; Jovin, T. M. *Science* **1988**, *241*, 551.
5. Rippe, K.; Fritsch, V.; Westhof, E.; Jovin, T. M. *EMBO J.* **1992**, *11*, 3777.
6. Marfurt, J.; Leumann, C. *Angew. Chem. Int. Ed.* **1998**, *37*, 175.
7. Fritzsche, H.; Akhebat, A.; Taillandier, E.; Rippe, K.; Jovin, T. M. *Nucleic Acids Res.* **1993**, *21*, 5085.
8. Li, H.; Peng, X.; Seela, F. *Bioorg. Med. Chem. Lett.* **2004**, *14*, 6031.
9. Müller, W.; Crothers, D. M. *J. Mol. Biol.* **1968**, *35*, 251.
10. Waring, M. J. *Annu. Rev. Biochem.* **1981**, *50*, 159.
11. Phillips, D. R.; Crothers, D. M. *Biochemistry* **1986**, *25*, 7355.
12. Graves, D. E.; Velea, L. M. *Curr. Org. Chem.* **2000**, *4*, 915.
13. Kamitori, S.; Takusagawa, F. *J. Mol. Biol.* **1992**, *225*, 445.
14. Robinson, H.; Gao, Y.-G.; Yang, X.-L.; Sanishvili, R.; Joachimiak, A.; Wang, A. H.-J. *Biochemistry* **2001**, *40*, 5587.
15. Hou, M.-H.; Robinson, H.; Gao, Y.-G.; Wang, A. H.-J. *Nucleic Acids Res.* **2002**, *30*, 4910.
16. Liu, C.; Chen, F.-M. *Biochemistry* **1996**, *35*, 16346.
17. Sobell, H. M.; Jain, S. C. *J. Mol. Biol.* **1972**, *68*, 21.
18. Chen, F.-M.; Sha, F.; Chin, K.-H.; Chou, S.-H. *Nucleic Acids Res.* **2003**, *31*, 4238.
19. Chen, F.-M. *Biochemistry* **1988**, *27*, 6393.
20. Chen, F.-M. *Biochemistry* **1992**, *31*, 6223.
21. Chen, F.-M.; Sha, F.; Chin, K.-H.; Chou, S.-H. *Nucleic Acids Res.* **2004**, *32*, 271.
22. Wadkins, R. M.; Jovin, T. M. *Biochemistry* **1991**, *30*, 9469.
23. Alexopoulos, E.; Jares-Erijman, E. A.; Jovin, T. M.; Klement, R.; Machinek, R.; Sheldrick, G. M.; Usón, I. *Acta Cryst.* **2005**, *D61*, 407.
24. Chin, K.-H.; Chen, F.-M.; Chou, S.-H. *Nucleic Acids Res.* **2003**, *31*, 2622.
25. Seela, F. Z. *Naturforschung* **1971**, *26b*, 875.
26. Wawra, H.; Müller, W.; Kratky, O. *Die Makromolekulare Chemie* **1970**, *139*, 83.
27. Veselkov, D. L.; Lantushenko, A. O.; Davies, D. B.; Veselkov, A. N. *Russ. J. Bioorg. Chem.* **2002**, *28*, 342.
28. Crothers, D. M.; Sabol, S. L.; Ratner, D. I.; Müller, W. *Biochemistry* **1968**, *7*, 1817.
29. Angerman, N. S.; Victor, T. A.; Bell, C. L.; Danyluk, S. S. *Biochemistry* **1972**, *11*, 2402.
30. Boger, D. L.; Fink, B. E.; Brunette, S. R.; Tse, W. C.; Hedrick, M. P. *J. Am. Chem. Soc.* **2001**, *123*, 5878.
31. Seela, F.; Steker, H. *Liebigs Ann. Chem.* **1984**, 1719.
32. Seela, F.; Driller, H. *Nucleic Acids Res.* **1985**, *13*, 911.
33. Wells, R. D.; Larson, J. E. *J. Mol. Biol.* **1970**, *49*, 319.
34. Seela, F.; Peng, X.; Li, H. *J. Am. Chem. Soc.* **2005**, *127*, 7739.
35. Tse, W. C.; Boger, D. L. *Acc. Chem. Res.* **2004**, *37*, 61.
36. Lewis, M. A.; Long, E. C. *Bioorg. Med. Chem.* **2006** (in press).

37. Brockmann, H.; Seela, F. *Chem. Ber.* **1971**, *104*, 2751.
38. Brockmann, H.; Schramm, W. *Tetrahedron Lett.* **1966**, *1*, 2331.
39. Seela, F.; Winkeler, H.-D.; Driller, H.; Menkhoff, S. *Nucleic Acids Res. Symp. Ser.* **1984**, 245.
40. Tor, Y.; Dervan, P. B. *J. Am. Chem. Soc.* **1993**, *115*, 4461.
41. Seela, F.; Menkhoff, S.; Behrendt, S. *J. Chem. Soc. Perkin Trans. 2* **1986**, 525.
42. Seela, F.; Peng, X. *Synthesis* **2004**, 1203.
43. Seela, F.; Wei, C. *Helv. Chim. Acta* **1999**, *82*, 726.
44. Seela, F.; He, Y.; Wei, C. *Tetrahedron* **1999**, *55*, 9481.
45. *User Manual of the DNA Synthesizer*. Applied Biosystems, Weiterstadt, Germany.
46. Fasman, G.D.; CRC Handbook of Biochemistry and Molecular Biology, 3rd ed.; Chemical Rubber Publishing Co.: Cleveland, OH, 1975; p 589.
47. McDowell, J. A.; Turner, D. H. *Biochemistry* **1996**, *35*, 14077.
48. Scatchard, G. *Ann. N.Y. Acad. Sci.* **1949**, *51*, 660.